

Articles

Long Chain Branching in Ethylene/Propylene Solution Polymerization Using Constrained Geometry Catalyst

Wen-Jun Wang, Shiping Zhu,* and Shin-Joon Park

Department of Chemical Engineering, McMaster University, Hamilton, Ontario L8S 4L7, Canada

Received February 4, 2000; Revised Manuscript Received May 23, 2000

ABSTRACT: Ethylene (E)/propylene (P) solution copolymerizations with low propylene ratios were carried out using constrained geometry catalyst, $[\text{C}_5\text{Me}_4(\text{SiMe}_2\text{N}^t\text{Bu})]\text{TiMe}_2$ (CGC), and *ansa*-zirconocene, *rac*-Et(Ind)₂ZrCl₂ (EBI), at 130–150 °C and 3.45×10^3 kPa. Ethylene/propylene copolymers with long chain branch (LCB) densities from 0.30 to 0.96 carbons per 10 000 carbons, molecular weight distributions close to 2, and narrow comonomer composition distributions were synthesized with CGC. Broad molecular weight and comonomer composition distributions were found in the EBI copolymers. Reactivity ratios showed that CGC was more active for propylene incorporation than EBI. Terminal group analysis indicated that more terminal unsaturation occurred with EBI than with CGC. Two additional types of terminal unsaturated groups, vinylidene with side group having more than three carbons (**2VD**) and trans-vinylene (**VE**), were found with EBI while the terminal vinyl (**V**) and vinylidene with methyl side group (**1VD**) were determined in both CGC and EBI copolymers. Long chain branch structures were formed by the **V** type macromonomer incorporation. The long chain branching rate constants were also estimated.

Introduction

Metallocene catalysts are very effective in olefin polymerization. They not only produce narrow molecular weight distribution olefin polymers at high activities, but also have good abilities for high α -olefin incorporation and good control over copolymer composition distributions. Moreover, metallocene catalysts with C_2 -symmetric and C_s -symmetric structures promote a stereoregular control in polyolefin formation. Extensive research has been carried out in ethylene (E)/propylene (P) copolymerization using C_{2v} , C_2 , and C_s -symmetric metallocenes.^{1–8} The C_s -symmetric metallocenes have the highest incorporation rates for propylene among the three, while the C_{2v} -symmetric ones give the lowest propylene incorporation. The specific catalysts retain their stereospecific controls.^{1–2}

Another organometallic catalyst with a half-sandwich structure called “constrained geometry catalyst” (CGC) has been developed to produce olefin polymers with long chain branch structures, which give an excellent combination of mechanical properties and processability for the resulting polymers. Its “constrained” structure permits an easy incorporation of high α -olefins and ethylene macromonomers.^{9,10} We studied solution ethylene homopolymerization and copolymerization with octene-1 at high temperature and pressure using CGC systems.^{11,12} The ethylene polymers and copolymers with octene-1 had narrow molecular weight distributions and narrow copolymer composition distributions.^{11–13} Recently, we reported a structural analysis on EP copolymer samples with about 30–60 mol % of

propylene fraction produced in a high-temperature continuous stirred-tank reactor (CSTR) using the CGC system. A large number of inverted propylene units and consecutive ethylene and propylene units were observed. The CGC did not have much control over the stereoregularity of propylene insertion.¹⁴

In this paper, long chain branching in ethylene/propylene copolymerization at low propylene contents was investigated in our high-temperature CSTR system using CGC. The copolymerization with a C_2 -symmetric *ansa*-zirconocene was also studied as a comparison. Polymer chain terminations were elucidated. The copolymer composition distributions were examined utilizing a segregation fractionation technique (SFT) by differential scanning calorimetry (DSC).

Experimental Section

Polymerization. CGC catalyst, $[\text{C}_5\text{Me}_4(\text{SiMe}_2\text{N}^t\text{Bu})]\text{TiMe}_2$ (Me: methyl; ^{*t*}Bu: isobutyl; C_5 : cyclopentadiene), and cocatalyst, tris(pentafluorophenyl)boron (TPFPB), were provided by Dow Chemical as 10 and 3 wt % solutions in Isopar E, respectively. *Ansa*-zirconocene, *rac*-Et(Ind)₂ZrCl₂ (Et, ethylene; Ind, 1-indenyl) (EBI) was from Boulder Scientific Co. Modified methylaluminoxane (MMAO-3A) was provided by Akzo-Nobel Corporation as 6.68 wt % aluminum in heptane. The catalysts and cocatalysts were used as received. Polymerization-grade ethylene with 240 ppm (in mol) of hydrogen and propylene from Matheson Gas were purified by CuO, Ascarite, CaH₂ and molecular sieves. Isopar E (an industrial solvent from Caledon Laboratories Ltd.) was dried over a mixture of molecular sieves from Aldrich and silica gel from Caledon Laboratories Ltd., and deoxygenated by sparging with ultrahigh purity nitrogen (99.999%) from Matheson Gas.

Polymerization runs were carried out in our high-temperature high-pressure CSTR system at 3.45×10^3 kPa and 130, 140, and 150 °C with a mean residence time (τ) of 4 min. The

* Corresponding author. Fax: (905)521-1350. E-mail: zhuship@mcmaster.ca.

Table 1. Experimental Conditions for Ethylene (E)/Propylene (P) Copolymerization in Continuous Stirred-Tank Reactor System Using CGC and EBI

run	$T/^\circ\text{C}$	$[\text{M}_\text{E}]_0/\text{d}/\text{M}$	$[\text{M}_\text{P}]_0/\text{d}/\text{M}$	$[\text{M}_\text{E}]/\text{d}/\text{M}$	$[\text{M}_\text{P}]/\text{d}/\text{M}$	f_P^e	$([\text{H}_2]_0/[\text{M}_\text{E}]_0)/10^6$
0	140	1.43	0	0.15	0	0	560
A1 ^a	130	1.26	0.18	0.23	0.05	0.173	240
A2 ^a	140	1.31	0.11	0.38	0.05	0.113	240
A3 ^a	140	1.16	0.20	0.39	0.11	0.220	240
A4 ^a	150	1.02	0.42	0.34	0.24	0.051	240
A5 ^a	150	1.24	0.18	0.24	0.11	0.310	240
B1 ^b	140	1.24	0.20	0.52	0.19	0.265	240
B2 ^c	140	0.88	0.55	0.29	0.51	0.637	240
B3 ^c	140	0.62	0.82	0.28	0.78	0.734	240

^a [CGC] = 15 μM ; [TPFPB] = 45 μM ; [MMAO] = 150 μM . ^b [EBI] = 1.5 μM ; [MMAO] = 1500 μM . ^c [EBI] = 2.5 μM ; [MMAO] = 2500 μM . ^d $[\text{M}_\text{E}]_0$, $[\text{M}_\text{E}]$, $[\text{M}_\text{P}]_0$, and $[\text{M}_\text{P}]$ are inlet ethylene, outlet ethylene, inlet propylene, and outlet propylene concentrations, respectively. ^e $f_\text{P} = [\text{M}_\text{P}]/([\text{M}_\text{E}] + [\text{M}_\text{P}])$.

details regarding the continuous solution polymerization reactor system setup can be found in our previous papers.^{11,12} The catalyst, cocatalyst, and propylene solutions were prepared and stored in separate tanks. The solvent, catalyst, and cocatalyst tanks were kept at a constant pressure of 2.05×10^2 kPa under the protection of nitrogen, and propylene tank was maintained at 1.34×10^3 kPa during the polymerization. The catalyst and cocatalyst concentrations, comonomer ratio, and mean residence time were controlled by adjusting feed rates of the four inlet streams and remained unchanged during the polymerization. The experimental conditions for each run are summarized in Table 1. The polymerization procedure was referred to the ethylene/octene-1 copolymerization.¹² During the polymerization, copolymers were collected and mixed with ethanol and then filtered, washed by methanol, and dried under vacuum.

Polymer Characterization. 75.4 MHz ^{13}C NMR spectra were acquired on a Bruker AC 300 pulsed NMR spectrometer with completed proton decoupling at 120 $^\circ\text{C}$. The samples were dissolved in a deuterated *o*-dichlorobenzene/1,2,4-trichlorobenzene (TCB) mixture with a concentration over 35 wt %. At least 6000 scans were applied for each acquisition to achieve good signal-to-noise. Figure 1 shows the spectra for samples A1, A4, B1, and B3 at chemical shifts from 50 to 10 ppm. The detailed assignments were given in our previous work.¹⁴

Molecular weight distributions were determined by a Waters-Millipore 150 C high-temperature SEC in TCB at 140 $^\circ\text{C}$ with a differential refractive index (DRI) detector. The universal calibration was performed using monodisperse TSK polystyrene standards from TOYO SODA Mfg.

Melting temperatures (T_m) and enthalpies of fusion (ΔH) of the copolymer samples were determined by a DuPont 910 differential scanning calorimeter (DSC) calibrated by indium standards. The copolymer samples (about 5 mg) were heated at 20 $^\circ\text{C}/\text{min}$ to 180 $^\circ\text{C}$, kept at 180 $^\circ\text{C}$ for 5 min, and then quenched to 20 $^\circ\text{C}$ at about 90 $^\circ\text{C}/\text{min}$. The T_m and ΔH values were acquired from the second heating cycle from 20 to 160 $^\circ\text{C}$ at a rate of 10 $^\circ\text{C}/\text{min}$.

A segregation fractionation technique (SFT)^{15,16} based on a stepwise crystallization by DSC was applied for the copolymer composition distribution measurement. After a preheating to 180 $^\circ\text{C}$ at about 120 $^\circ\text{C}/\text{min}$, a sample was then cooled to just above melting point of the sample, and successively annealed at six temperatures with an interval of 6 $^\circ\text{C}$. The time interval from one annealing temperature to another was 150 min. For sample, A2 with T_m of 106 $^\circ\text{C}$, six annealing temperatures of 128, 122, 116, 110, 98, and 92 $^\circ\text{C}$ were utilized. Lower annealing temperatures were employed for the polymers with higher propylene contents. A second heating cycle following the annealing step was used for the acquisition of melting thermogram of the fractionated copolymers. The scanning rate was 5 $^\circ\text{C}/\text{min}$.

Results and Discussion

Copolymerization Kinetics. Table 2 presents conversion, polymerization rate, and catalyst activity data, as well as propylene composition (F_P) and molecular weight distribution for the CGC and EBI copolymeri-

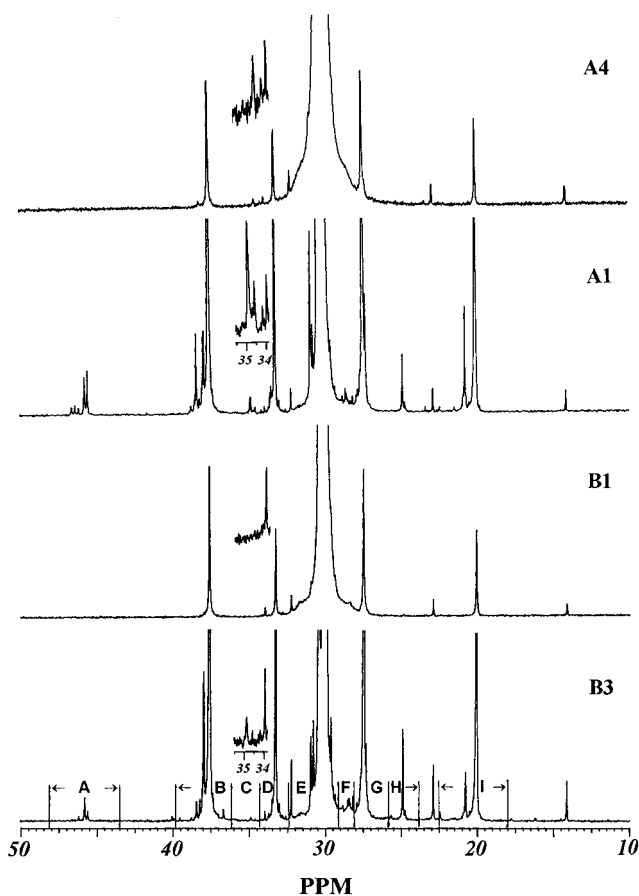


Figure 1. ^{13}C NMR spectra of ethylene/propylene copolymers from 50 to 10 ppm. CGC polymer samples A4 and A1 have propylene mole fractions (F_P) of 0.007 and 0.111. EBI samples B1 and B3 have F_P values of 0.014 and 0.110.

zation systems. In comparison with ethylene homopolymerization using the CGC (run 0),¹¹ the ethylene/propylene systems had lower polymerization rates and activities, which were inversely influenced by propylene incorporation. The activities changed from 7.27 kg of polymer/g of catalyst (or 15 600 kg of polymer/([M]·mol of Ti)) to 5.19 kg of polymer/g of catalyst (or 3400 kg of polymer/([M]·mol of Ti)) at 140 $^\circ\text{C}$ when 10.3 mol % of propylene was incorporated (A3). The GPC measurement showed that the copolymerization using CGC produced low molecular weight polymers. At 140 $^\circ\text{C}$ the weight-average molecular weight (M_w) decreased from 1.04×10^5 to 4.40×10^4 (A3) with F_P of 0.103. The GPC measurement also showed that the propylene incorporation did not broaden molecular weight distribution (MWD) of the CGC copolymers. The MWD's were close to 2 for all CGC samples.

Table 2. Results of Continuous Solution Copolymerization of Ethylene/Propylene Using CGC and EBI^a

run	f_P	F_P	$X/\%$	$X_E/\%$	$X_P/\%$	$R_P/10^3$ M/s	$M_w/10^{-4}$	M_w/M_n	activity/(kg of polymer/g of catalyst)	activity/(10^{-3} kg of polymer/[M] \times mol of metal) ^b
0	0	0	89.3	89.3	0	5.31	10.4	2.0	7.27	15.6
A1	0.173	0.111	79.8	81.4	72.3	4.80	4.25	2.2	6.95	8.02
A2	0.113	0.064	69.4	71.0	56.7	4.13	7.23	2.0	5.84	4.48
A3	0.220	0.103	62.1	66.6	44.7	3.60	4.40	1.9	5.19	3.40
A4	0.051	0.007	81.4	82.4	39.4	4.60	10.3	2.1	6.33	8.39
A5	0.310	0.072	73.7	80.8	42.2	4.48	4.04	2.2	6.37	6.05
B1	0.265	0.014	47.4	57.6	5.2	3.01	4.66	2.6	32.5	19.1
B2	0.637	0.061	38.2	67.2	7.0	2.62	2.72	3.6	17.4	15.2
B3	0.734	0.110	21.4	54.2	5.0	1.57	2.14	4.0	10.6	6.96

^a Key: X , conversion; R_P , copolymerization rate; M_w , weight-average molecular weight; M_w/M_n , molecular weight distribution. ^b Metal = Ti for runs 0 and A1–A5 and Zr for runs B1–B3.

Three runs (B1–B3) with f_{P0} (inlet propylene mole ratio) of 0.139 (B1), 0.383 (B2), and 0.571 (B3) were also carried out in the CSTR using the EBI systems. The catalyst activities at 140 °C were 10.6–32.5 kg of polymer/g of catalyst (6960–19 100 kg of polymer/([M]·mol of Zr)), which were about 2–5 times that of the CGC ones. Molecular weights were lower than those of the CGC copolymers, and also decreased with increasing propylene incorporation. Broad molecular weight distributions were observed in the EBI copolymers. MWD changed from 2.6 to 4.0 as F_P varied from 0.014 to 0.110. Considering that EBI was dispersed in Isopar E (a poor solvent for EBI) as fine particles (aggregate of the EBI molecules), the polymer chain growth on the active sites improved the solubility of EBI and thus made the activated centers to leave from the aggregate. The difference in their activation times for different EBI molecules broadened the molecular weight distribution of the copolymers.

The reactivity ratios (r_E and r_P) for the CGC system at 140 °C were reported in our previous work.¹⁷ r_E and r_P were 4.33 and 0.377, respectively. From the copolymer compositions (F_P) and propylene mole fractions (f_P) for the EBI system shown in Table 2, the r_E and r_P values were estimated at 36.5 and 0.265 using the Gause–Newton algorithm.¹² It can be seen that CGC is more active for propylene incorporation than EBI.

Comonomer Sequence Distribution. The assignments for each resonance and integral in the ¹³C NMR spectra were given in our previous work.¹⁴ As few inverted propylene units were present in the copolymers, we did not consider their contributions to the comonomer sequence distribution. The resonance areas of methylene and methine carbons were used for the calculations. The relationships between the triad distributions and the integrals are¹⁸

$$kI_A = p(\text{PPP}) + \frac{1}{2}p(\text{PPE} + \text{EPP}) \quad (1)$$

$$kI_B = p(\text{PEP}) + \frac{1}{2}p(\text{PEE} + \text{EEP}) + p(\text{EPE}) + \frac{1}{2}p(\text{PPE} + \text{EPP}) \quad (2)$$

$$kI_D = p(\text{EPE}) \quad (3)$$

$$kI_E = 2p(\text{EEE}) + p(\text{PPE} + \text{EPP}) + \frac{1}{2}p(\text{PEE} + \text{EEP}) \quad (4)$$

$$kI_G = p(\text{PEE} + \text{EEP}) \quad (6)$$

$$kI_H = p(\text{PEP}) \quad (7)$$

where k is the NMR signal proportionality constant, I s are the integral areas with their subscripts denoting the integral ranges in Figure 1, and $p(\text{ijk})$'s are the triad ijk distributions.

As the propylene levels in the copolymers were low, area F did not fairly separate from area E. The combination area of E and F was used for the calculation. Therefore

$$p(\text{PPP}) = k(I_A - I_B + I_D + \frac{1}{2}I_G + I_H) \quad (8)$$

$$p(\text{PPE} + \text{EPP}) = k(2I_B - 2I_D - I_G - 2I_H) \quad (9)$$

$$p(\text{PEP}) = k(I_H) \quad (10)$$

$$p(\text{PEE} + \text{EEP}) = k(I_G) \quad (11)$$

$$p(\text{EPE}) = k(I_D) \quad (12)$$

$$p(\text{EEE}) = \frac{1}{2}k(I_E + I_F - I_A - I_B + I_D + I_H) \quad (13)$$

The triad distributions were calculated using eqs 8–13 and were given in Table 3. For the copolymers with low propylene content of 0.01 (samples A4 and B1), the PPP, PPE + EPP, and PEP triads cannot be identified. Comparing the CGC copolymers with the EBI counterparts at the same F_P (0.06 for A2 and B2, and 0.11 for A1 and B3), we observed that the CGC copolymers had more PPP and EEE triads than the EBI copolymers. At the same 0.11 propylene incorporation, there were 0.013 of PPP and 0.729 of EEE triad in the CGC copolymer corresponding 0.003 and 0.706 in the EBI copolymer. This indicated that the monomer insertion in the CGC catalyst had more long runs of the same monomer types.

Terminal Unsaturation. In metallocene olefin polymerization, β -hydride elimination, chain transfer to monomer, and alkyl elimination are major termination mechanisms to form unsaturated chain end groups. We studied ethylene homopolymerization and ethylene/octene-1 copolymerization using the CGC system, and found that chain transfer to monomer was the major chain termination in the ethylene homopolymerization,¹¹ and that the octene-1 incorporation enhanced the chain termination in the ethylene/octene-1 copolymerization.¹² Figure 2a shows the ¹³C NMR spectra from 155 to 105 ppm for samples A2, A3, and A4. The subscripts S, T, and Q in Figure 2 denote the secondary, tertiary, and quaternary carbons, respectively. In the

Table 3. Comonomer Sequence Distributions in CGC and EBI Ethylene/Propylene Copolymers

sample	$T/^\circ\text{C}$	F_P	$p(\text{PPP})$	$p(\text{PPE} + \text{EPP})$	$p(\text{PEP})$	$p(\text{PEE} + \text{EEP})$	$p(\text{EPE})$	$p(\text{EEE})$
A1	130	0.111	0.013	0.008	0.014	0.154	0.082	0.729
A2	140	0.064	0.005	0.001	0.006	0.084	0.057	0.848
A3	140	0.103	0.012	0.004	0.014	0.144	0.078	0.748
A4	150	0.007	0.000	0.000	0.000	0.014	0.007	0.978
A5	150	0.072	0.005	0.005	0.008	0.099	0.061	0.823
B1	140	0.014	0.000	0.000	0.000	0.028	0.014	0.958
B2	140	0.061	0.001	0.002	0.007	0.089	0.060	0.840
B3	140	0.110	0.003	0.009	0.018	0.166	0.099	0.706

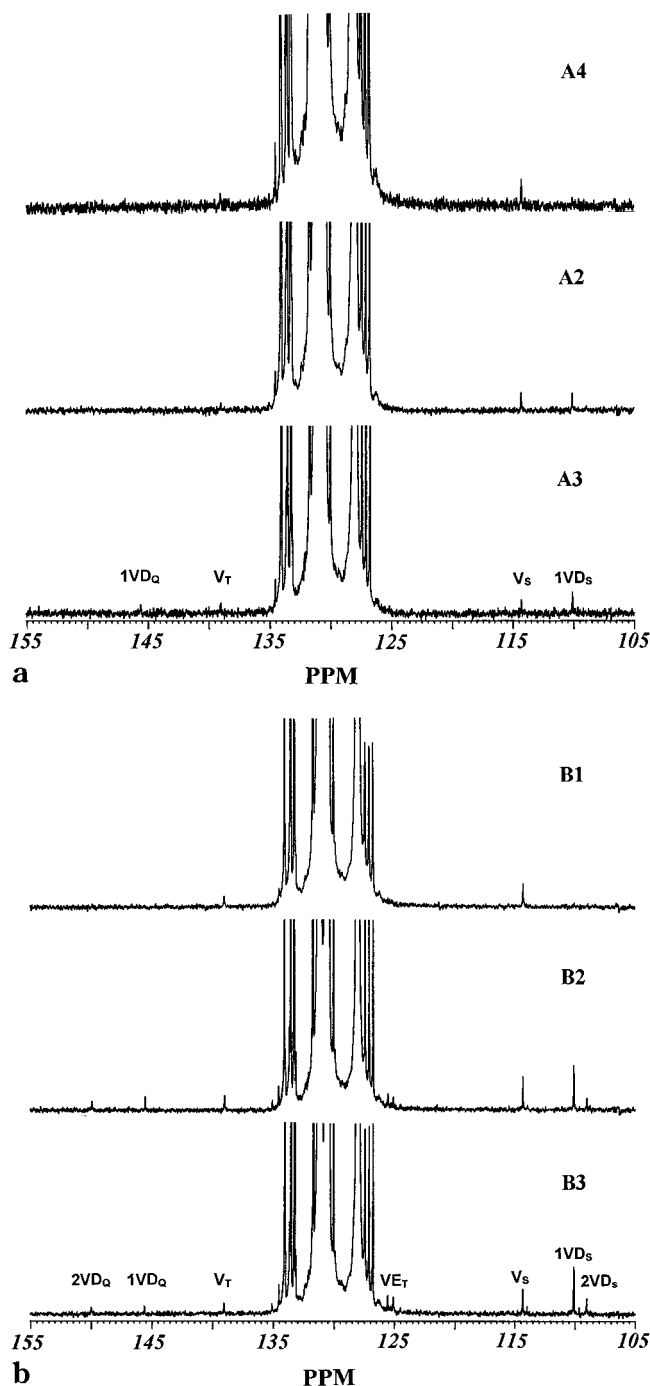
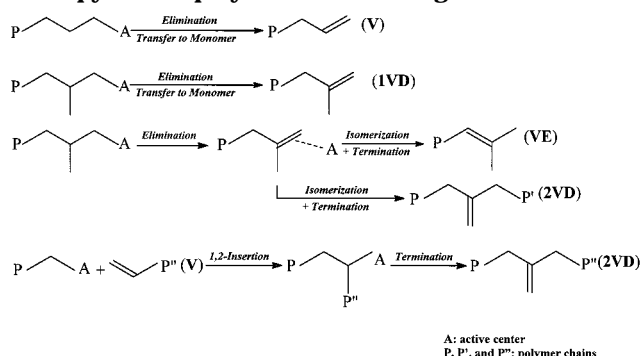


Figure 2. ^{13}C NMR spectra of ethylene/propylene copolymers from 155 to 105 ppm: (a) CGC samples A4, A2, and A3 with F_P of 0.007, 0.064, and 0.103; (b) EBI samples B1, B2, and B3 with F_P of 0.014, 0.061, and 0.110.

copolymerization at low propylene ratios only terminal vinyl groups (**V**) (chemical shifts at 139.0 and 114.3 ppm assigned to the tertiary ($=\text{CH}-$) and secondary ($=\text{CH}_2$) carbons)¹⁹ were observed in sample A4. The terminal

Scheme 1. Mechanisms for the Formation of Unsaturated Chain End Groups in Ethylene/Propylene Copolymerization Using CGC and EBI



vinylidene groups with methyl side group (**1VD**), having resonances at 145.5 and 110.1 ppm assigned to the quaternary ($=\text{C}<$) and secondary carbons,²⁰ were detected in samples A2 and A3 with the propylene contents higher than A1. From Figure 2a, we can see more **1VD** than **V** in sample A3 (compared to sample A2), indicating propylene enhanced the chain transfer to monomer.

The ^{13}C NMR spectra for the unsaturated groups in samples B1 to B3 are given in Figure 2b. The **V** and **1VD** groups were also observed in the EBI copolymers. Higher unsaturated resonance intensities in Figure 2b than in Figure 2a at comparable F_P levels indicated high termination rates in the copolymerization with EBI than with CGC. In addition to the terminal **V** and **1VD** groups, other double bonds were also found in the EBI copolymers. The resonances at 109 and 150 ppm appeared in samples B2 and B3, and the intensities increased with increasing the propylene content. These chemical shifts can be assigned to terminal vinylidene with side group having more than three carbons (**2VD**).¹² The **2VD** structure might also be considered as an internal vinylidene if the side group were a main chain. The adjacent methylene units to **2VD** group can also be identified in the copolymers with $\alpha\text{-CH}_2$ of 35.8 ppm and $\beta\text{-CH}_2$ of 27.9 ppm.^{12,15} Because the carbon numbers for the side group of **2VD** unit could not be identified, the following two possible reaction pathways were believed to be responsible for **2VD** unit formation as shown in Scheme 1. The **2VD** unit might result from a 1,2-insertion of polymer with **V**-type unit followed by a β -hydride elimination and/or chain transfer to monomer. In this case the side group of **2VD** unit had a long carbon chain. Alternatively, an isomerization after a β -hydride elimination might also form the **2VD** unit. This **2VD** unit thus formed should have a short carbon unit.

As a strong resonance of phenyl group in TCB appeared from 135 to 126 ppm, resonance peaks of double bond groups in this range were overlaid. However, resonances at 125.5 and 125.0 ppm were still

Table 4. Summary of ^{13}C NMR Data for CGC Ethylene/Propylene Copolymers

sample	$T/^\circ\text{C}$	LCBD/ 10^4	TVD/ 10^4	[P $^{2-}$]/ 10^4		
				M	$k_{\text{PL}}/k_{\text{PE}}^a$	$k_{\text{PL}}/k_{\text{PP}}^a$
0	140	0.35	0.65	1.66		
A1	130	0.49	1.48	3.61	0.10	0.31
A2	140	0.47	2.20	4.50	0.12	0.32
A3	140	0.30	1.64	2.98	0.14	0.38
A4	150	0.63	1.38	3.07		
A5	150	0.96	2.31	5.16	0.15	0.34

^a $k_{\text{EL}}/k_{\text{EE}} = 0.069$ (130 $^\circ\text{C}$), 0.081 (140 $^\circ\text{C}$), and 0.096 (150 $^\circ\text{C}$) from ref 11; $r_{\text{E}} = 2.89$, $r_{\text{P}} = 0.324$ (130 $^\circ\text{C}$); $r_{\text{E}} = 4.33$, $r_{\text{P}} = 0.377$ (140 $^\circ\text{C}$); and $r_{\text{E}} = 6.36$, $r_{\text{P}} = 0.436$ (150 $^\circ\text{C}$) from ref 17.

detected, which were assigned to the trans-vinylene chain ends (**VE**).²¹ An evidence from peaks at 25.6, 17.6, and 16.2 ppm assigned to the methyl groups of the **VE** groups gave a further support.^{21,22} An isomerization after β -hydride elimination is believed to form the terminal **VE**. The same types of termination reactions were also reported in propylene solution homopolymerization using *ansa*-zirconocene.²³ The formation of **1VD**, **2VD**, and **VE** units in the EBI copolymers were most likely due to propylene incorporation.

Long Chain Branching. In ethylene homopolymerization using CGC, we found that long chain branching (LCB) occurred by the insertion of polyethylene macromonomer right after it was generated at the same active site. This branch structure has a detectable chemical shift in 34.5 ppm assigned to $\alpha\text{-CH}_2$ (methylene carbons adjacent to branched methine carbons). Figure 1 gives some spectra for the CGC and EBI copolymer samples. The chemical shift in 34.5 ppm was clearly observed in the CGC copolymers, but not in the EBI copolymers. It indicated that the long chain branches are present in the ethylene/propylene copolymers prepared by CGC.

Two types of terminal unsaturated units, **V** and **1VD**, were identified in CGC copolymers. The LCB by the incorporation of the terminal **V** unit shows resonances at 34.5 ($\alpha\text{-CH}_2$) and 38.2 ppm (methine). As a methyl group existed in the **1VD** group, an incorporation of the **1VD** will produce a LCB structure with a quaternary carbon. The chemical shifts at 25.2, 40.3, and 29.1 ppm, which are assigned to the methyl carbon adjacent to branched quaternary carbon, $\alpha\text{-CH}_2$, and branched quaternary carbon,²² should be detectable. In the present copolymers, resonance at 29.1 ppm could not be identified due to an overlap of isolated methylene carbons. However, no resonance at chemical shifts of 25.2 and 40.3 ppm suggested that the terminal **1VD** group did not contribute to the LCB formation.

The following are the elementary reactions for monomer propagation and long chain branching during the copolymerization with CGC, in which the effect of penultimate monomer units on the activity of active centers is neglected.

Propagation:



Long Chain Branching:



where $[\text{P}^{2-}]$ is the concentration of copolymer with terminal **V** group, $[\text{A}_\text{E}]$ and $[\text{A}_\text{P}]$ are the concentrations of the active centers with the last inserted monomer unit being ethylene (A-E) and propylene (A-P), and $[\text{M}_\text{E}]$ and $[\text{M}_\text{P}]$ are ethylene and propylene outlet concentrations, respectively. k_{ij} 's and R_{ij} 's denote their reaction rate constants and reaction rates.

The long chain branch units were generated via the competition between monomer propagation and macromonomer incorporation, that is, were proportional to the ratio of ($R_{\text{EL}} + R_{\text{PL}}$) over ($R_{\text{EE}} + R_{\text{EP}} + R_{\text{PE}} + R_{\text{PP}}$). Under the long chain assumption applied to the cross propagation rates, the following relationship between long chain branch density (LCBD, the number of branched units per carbon) and propagation rate coefficient can be derived

$$\text{LCBD} = \frac{(k_{\text{EL}}/k_{\text{EE}}r_{\text{E}}[\text{M}_\text{E}] + k_{\text{PL}}/k_{\text{PE}}[\text{M}_\text{P}])[\text{P}^{2-}]}{2r_{\text{E}}[\text{M}_\text{E}]^2 + 5[\text{M}_\text{E}][\text{M}_\text{P}] + 3r_{\text{P}}[\text{M}_\text{P}]^2} \quad (20)$$

where the concentration of terminal vinyl group $[\text{P}^{2-}]$ can be estimated from its density TVD (the number of terminal vinyl units per carbon):

$$[\text{P}^{2-}] = \{2([\text{M}_\text{E}]_0 - [\text{M}_\text{E}]) + 3([\text{M}_\text{P}]_0 - [\text{M}_\text{P}])\}\text{TVD} \quad (21)$$

We have determined the $k_{\text{EL}}/k_{\text{EE}}$ values of 0.081–0.15 at a temperature range from 140 to 190 $^\circ\text{C}$.¹¹ The $k_{\text{PL}}/k_{\text{PE}}$ values can therefore be estimated from eq 20.

LCBD, TVD, and $[\text{P}^{2-}]$ values are summarized in Table 4. The LCBD values are from 0.30 to 0.96 carbons per 10 000 carbons. In ethylene homopolymerization we synthesized polyethylene (PE) samples with LCBD up to 0.44 carbons/10 000 carbons.¹¹ The LCBD's in the CGC copolymers are higher than those in the CGC PE's. As sample A4 was synthesized at a very low propylene concentration at 150 $^\circ\text{C}$, the macromonomer propagation on the A-P active center could be neglected. The $k_{\text{EL}}/k_{\text{EE}}$ was, therefore, estimated 0.098, which was the same value as that we obtained from the ethylene homopolymerization.¹¹ From eq 20, the $k_{\text{PL}}/k_{\text{PE}}$ and $k_{\text{PL}}/k_{\text{PP}}$ ($= (k_{\text{PL}}/k_{\text{PE}})/r_{\text{P}}$) were calculated as shown in Table 4. The $k_{\text{PL}}/k_{\text{PE}}$ values were 0.10 to 0.15 and the $k_{\text{PL}}/k_{\text{PP}}$ were from 0.31 to 0.35 at 130 to 150 $^\circ\text{C}$. Both $k_{\text{PL}}/k_{\text{PE}}$ and $k_{\text{PL}}/k_{\text{PP}}$ values were higher than the $k_{\text{EL}}/k_{\text{EE}}$ ones. This also explained why higher LCBD was observed in the EP copolymers than in PE.

Segregation Fractionation (SFT) Analysis. The comonomer incorporation influences crystallization behaviors of the ethylene copolymer. The DSC thermograms for three CGC copolymers with F_{P} of 0.01 (A4), 0.06 (A2), and 0.11 (A1) and three EBI samples (B1, B2, and B3) having the same F_{P} values are presented in Figure 3, parts a and b. The enthalpies and melting points calculated from peaks of the thermograms are

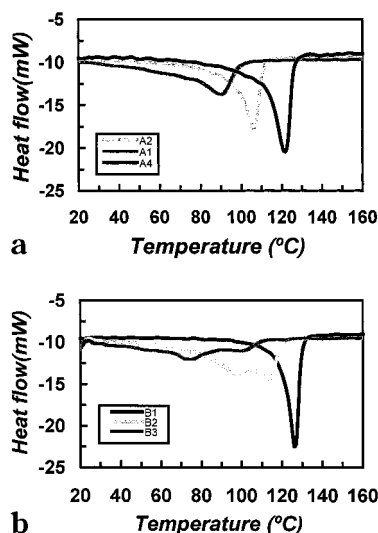


Figure 3. DSC thermograms for CGC and EBI copolymers: (a) CGC samples A4, A2, and A1 with F_p of 0.007, 0.064, and 0.111; (b) EBI samples B1, B2, and B3 with F_p of 0.014, 0.061, and 0.110.

Table 5. Melting Temperatures and Enthalpies of CGC and EBI Ethylene/Propylene Copolymers

run	$T_m/^\circ\text{C}$	$\Delta H/(\text{J/g})$
0	132.6	176
A1	90.2	96
A2	106	122
A3	92	97
A4	128.6	220
A5	103.4	147
B1	126.4	179
B2	98.1, 113.3	168
B3	74.9, 99.4	104

given in Table 5. A single endothermic peak was observed in the CGC copolymers and EBI sample B1, and the endothermic curves with dual peaks were seen in samples B2 ($F_p = 0.061$) and B3 ($F_p = 0.110$). Two melting peak temperatures were found at 98.1 and 113.3 °C for sample B2, and 74.9 and 99.4 °C for B3. The DSC traces became broader with higher propylene contents in the copolymers. The zirconocene copolymers had a significant line broadening compared to the CGC ones.

We plotted the melting temperature with the propylene mole fraction (F_p) for the CGC samples in Figure 5. A linear relationship was observed. The EBI samples were also plotted in the figure. B1 was on the line. However, B2 and B3 departed from the line, indicating the presence of two distinguished EP populations in the samples. The fraction and composition of each population can be estimated using the relative distances of the points from the line. For example, the compositions of the two populations in B2 are B2(1) with $F_p = 0.087$ and B2(2) with $F_p = 0.048$. The fraction of the former is $(0.061 - 0.048)/(0.087 - 0.048) = 0.33$.

In this work, the M_w ranged from 4×10^4 to 10×10^4 . The effect of molecular weight on this linear T_m and F_p relationship was minor. Therefore, a segregation fractionation technique (SFT) using DSC, a successive annealing at different temperatures starting above melt temperature to fractionate the polymer (mainly based on the lamellar thickness), was used to examine the comonomer composition distribution.^{15–16}

Three CGC (A1, A2, and A4) and three EBI samples (B1, B2, and B3) were determined by the SFT DSC. Their thermograms are given in Figure 5, parts a and

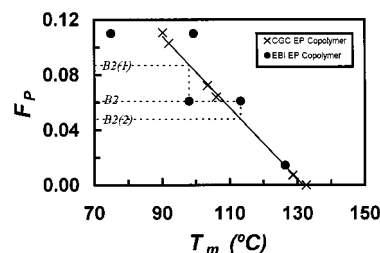


Figure 4. Relationship between melting temperature (T_m) and propylene mole fraction (F_p) for CGC and EBI copolymers.

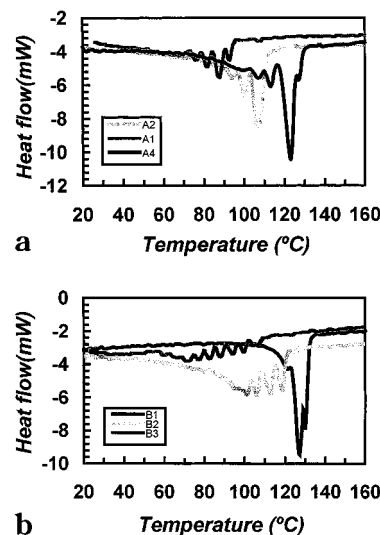


Figure 5. Segregation fractionation technique (SFT) DSC thermograms for CGC and EBI copolymers: (a) CGC samples A4, A2, and A1 with F_p of 0.007, 0.064, and 0.111; (b) EBI samples B1, B2, and B3 with F_p of 0.014, 0.061, and 0.110.

b. For the samples with low propylene contents (samples A4 and B1), there was one dominant peak (128.6 °C for A4 and 126.4 °C for B1), and two to three melting peaks ranged from 100 to 115 °C. With the increment of the propylene content, the SFT DSC curves became broader and more melting peaks appeared. About six melting peaks from 70 to 100 °C were acquired for samples A1 and B3. The SFT thermograms also showed that there was one dominant melting peak in all CGC copolymers. However, multiple peaks with similar intensities were observed in the EBI copolymers with the propylene contents of 0.061 (B2) and 0.110 (B3). For the copolymers with similar propylene composition, the melting peaks with broad temperature range were found in the EBI copolymers. Sample B3 had melting peaks from 68 to 104 °C while the melting peaks for sample A1 ranged from 69 to 93 °C, indicating narrow comonomer composition distributions in the CGC copolymers.

Conclusions

Long chain branching in continuous solution copolymerization of ethylene with propylene using the CGC was studied at low propylene ratios. A series of parallel copolymerizations were carried out using the EBI. LCB ethylene/propylene copolymers with LCB of 0.30–0.96 carbons per 10 000 carbons and a molecular weight distribution close to 2 were synthesized by the CGC system. The EBI catalyst had higher activity than the CGC and produced EP copolymers with broader molecular weight distributions from 2.6 to 4.0. More unsaturated terminations occurred with EBI than with the CGC

system. Four types of terminal unsaturated units, vinyl (**V**), vinylidene with methyl side group (**1VD**) and side group having more than three carbons (**2VD**), and trans-vinylene chain ends (**VE**) were observed in the EBI copolymers while only the **V** and **1VD** groups were found in the CGC copolymers. The **V** type macromonomer incorporation produced LCB structures. The long chain branching rate constant k_{PL}/k_{PE} 's were 0.10 to 0.15 and k_{PL}/k_{PP} 's were from 0.31 to 0.35 at 130 to 150 °C. The reactivity ratios r_E and r_P for the EBI catalyst at 140 °C were estimated as 36.5 and 0.265. Compared to the reactivity ratios 4.33 and 0.377 for CGC, the EBI was much less active for propylene incorporation. The study on monomer sequence distribution showed more PPP and EEE triads in the CGC copolymers than in the EBI ones. The segregation fractionation technique (SFT) revealed narrow comonomer composition distributions in the CGC copolymers.

Acknowledgment. The authors are grateful to the National Sciences and Engineering Research Council of Canada (NSERC) for funding support.

References and Notes

- (1) Uozumi, T.; Soga, K. *Makromol. Chem.* **1992**, *193*, 823.
- (2) Zambelli, A.; Grassi, A.; Galimberti, M.; Mazzocchi, R.; Piemontesi, F. *Makromol. Chem., Rapid Commun.* **1991**, *12*, 523.
- (3) Galimberti, M.; Destro, M.; Fusco, O.; Piemontesi, F.; Camurati, I. *Macromolecules* **1999**, *32*, 258.
- (4) Ewen, J. A. In *Catalytic Polymerization of Olefins*; Keii, T., Soga, K., Eds.; Kodansha: Tokyo, 1986; p 271.
- (5) Kaminsky, W.; Miri, M. *J. Polym. Sci., Polym. Chem. Ed.* **1985**, *23*, 2151.
- (6) Arndt, M.; Kaminsky, W.; Schauwienold, A.-M.; Weingarten, U. *Macromol. Chem. Phys.* **1998**, *199*, 1135.
- (7) Jin, J.; Uozumi, T.; Sano, T.; Teranishi, T.; Soga, K.; Shiono, T. *Macromol. Rapid Commun.* **1998**, *19*, 337.
- (8) Chien, J. C. W.; De, D. *J. Polym. Sci., Polym. Chem. Ed.* **1991**, *29*, 1585.
- (9) Lai, S. Y.; Wilson, J. R.; Knight, G. W.; Stevens, J. C.; Chum, P. W. S. (to Dow Chemical Co.) Elastic substantially linear olefin polymers, U.S. Patent 5,272,236, 1993.
- (10) Brant, P.; Canich, J. A. M. (to Exxon Chemical Patents Inc.) Ethylene/Longer α -olefin copolymers, W.O. Patent 93/12,151, 1993/U.S. Patent 5,475,075, 1993.
- (11) Wang, W.-J.; Yan, D.; Zhu, S.; Hamielec, A. E. *Macromolecules* **1998**, *31*, 8677.
- (12) Wang, W.-J.; Kolodka, E. B.; Zhu, S.; Hamielec, A. E. *J. Polym. Sci., Polym. Chem. Ed.* **1999**, *37*, 2949.
- (13) Wang, W.-J.; Kolodka, E.; Zhu, S.; Hamielec, A. E.; Kostanski, L. K. *Macromol. Chem. Phys.* **1999**, *200*, 2146.
- (14) Wang, W.-J.; Zhu, S. *Macromolecules* **2000**, *33*, 1157.
- (15) Pietikainen, P.; Starck, P.; Seppala, J. V. *J. Polym. Sci., Polym. Chem. Ed.* **1999**, *37*, 2379.
- (16) Lehtinen, C.; Starck, P.; Lofgren, B. *J. Polym. Sci., Polym. Chem.* **1997**, *35*, 307.
- (17) Park, S.-J.; Wang, W.-J.; Zhu, S. *Macromol. Chem. Phys.* **2000**, in press.
- (18) Randall, J. C. *J. Macromol. Sci.—Rev. Macromol. Chem. Phys.* **1989**, *C29*, 201.
- (19) Couperus, P. A.; Clague, A. D. H.; van Dongen, J. P. C. M. *Org. Magn. Reson.* **1976**, *8*, 426.
- (20) Cheng, H. N.; Smith, D. A. *Macromolecules* **1986**, *19*, 2065.
- (21) Kolbert, A. C.; Didier, J. G.; Xu, L. *Macromolecules* **1996**, *29*, 8591.
- (22) Nemes, S.; Borbely, J. *J. Macromol. Sci.—Pure Appl. Chem.* **1997**, *A34*, 2355.
- (23) Carvill, A.; Zetta, L.; Zannoni, G.; Sacchi, M. C. *Macromolecules* **1998**, *31*, 3783.

MA000209X